Fermilab FERMILAB-Conf-01/363-E December 2001

Recent Results from CDF and Status of CDF-II

C. Pagliarone

I.N.F.N. of Pisa

via Livornese, 1291 - 56010 S. Piero a Grado (PI) - ITALY

E-mail: pagliarone@fnal.gov

(ON THE BEHALF OF THE CDF COLLABORATION)

Abstract

The CDF detector collected during 1992-95 (Run I) a data sample of 110 pb^{-1} $p\bar{p}$ collisions at a center of mass energy $\sqrt{s} = 1.8$ TeV. A large variety of physical studies and measurements has been performed using these data. The current paper wants to review results obtained using this data sample as well as discuss the CDF-II upgrades and physical potential of the upgraded CDF Detector (CDF-II) in the Run II.

1 Tevatron Collider

The Fermilab Tevatron Collider has undergone in the past few years a whole series of upgrades to increase the instantaneous luminosity and to improve the bunch structure. During the Run II the machine is expected to deliver a luminosity of up to $2.0 \times 10^{32}\ cm^{-2}s^{-1}$ at a center of mass energy $\sqrt{s} = 2\ TeV$ to each of the two collider experiments: CDF and DØ. During the present Run IIa the Tevatron will mainly operate much like in the Run Ib with a higher integrated luminosity mostly coming from an increase in the number of bunches and slightly higher proton and antiproton bunch intensities ($N_{\bar{p}} \sim 0.5 \times 10^{32}\ cm^{-2}s^{-1}$). The goal of the Run IIa is to achieve an integrated luminosity of $\int \mathcal{L}\, dt \sim 2fb^{-1}$. The bunch structure of Tevatron Collider has been changed. Indeed, we passed from the $6p \times 6\bar{p}$ bunches of the Run I, to $36p \times 36\bar{p}$ and sometime in the future we will go to $140p \times 121\bar{p}$, with an inter-bunch gap of 132 ns. The increased number of bunches, in the last described scenario, will help to decrease the average number of interactions per bunch crossing. This is important if we want to improve the detector performances.

The replacement of the Main Ring with the Main Injector as the injection source for the Tevatron, leads to an increased number of protons per store and at the same time eliminates a source of background for the detectors. Several upgrades also increase the number of antiprotons per store. New Main Injector creates antiproton beam with higher intensity and energy than in the Run I. In addition, the plan is to recycle 'unused' antiprotons at the end of a collider store rather than dump them. Finally, the collider center of mass energy has been increased from 1.8 TeV to the present energy of 2.0 TeV.

Collider Parameters	Tevatron Run Ib	Tevatron Run IIa	Tevatron Run IIa	Tevatron Run IIb
Energy per beam (TeV)	0.9 TeV	1.0 TeV	1.0 TeV	1.0 TeV
Number of bunches	$6p \times 6\bar{p}$	$36p \times 36\bar{p}$	$140p \times 103\bar{p}$	$140p \times 103\bar{p}$
Number of p per bunch	2.3×10^{11}	2.7×10^{11}	2.7×10^{11}	2.7×10^{11}
Number of $\bar{p}$ per bunch	5.5×10^{10}	3.0×10^{10}	4.0×10^{10}	1.1×10^{11}
Bunch Separation (ns)	3500 ns	396 ns	132 ns	132 ns
Crossing Angle (μRad)	0 μRad	0 μRad	136 μRad	136 μRad
Typical Luminosity ($cm^{-2}s^{-1}$)	0.16×10^{31}	0.86×10^{32}	2.1×10^{32}	5.2×10^{32}

Table 1: *Operational performance of Tevatron in Run I and goals for Run II (Run Ib is the Tevatron 1993-1996 data-taking Run).*

Table 1 summarizes the operational performance of the Tevatron in the Run I and goals for the Run II. Tevatron Run II started in march 2001 and is scheduled to last until 2006. Both Tevatron Collider Detectors have been improved in order to operate with the new machine performance that means mainly with an increased instantaneous luminosity as well as the critical bunch spacing structure. A detailed description of the CDF and DØ detector upgrades may be found in the following documents [1, 2].

2 The CDF Detector

The Collider Detector at Fermilab is a 5000 ton multi-purpose particle physics experiment [3] dedicated to the study of proton-antiproton collisions at the Fermilab Tevatron collider. It was designed, built and operated by a team of physicists, technicians and engineers that now spans 44 institutions and includes, approximately, more than 500 members. The history of the experiment goes back over 20 years. Table 2 gives some details of this long path. The CDF detector has been recently upgraded [1] in order to be able to operate at the high radiation and high crossing rate of the Run II Tevatron environment. In addition, there have been several upgrades to improve the sensitivity of the detector to specific physics tasks such as heavy flavor physics, Higgs boson searches and many others. Figure 1 (left) shows an isometric cutaway view of the final configuration of the CDF experiment.

The central tracking volume of the CDF experiment has been replaced entirely with new detectors (see Figure 1, right), the central calorimeters has not been changed, the muon system has been mainly improved in coverage. These upgrades can be summarized as follow:

- A new **silicon system** done of 3 different tracking detector subsystems:
  Layer00 – a layer of silicon detectors installed directly on the beam pipe to increase impact parameter resolution.
  Silicon Vertex Detector (SVX II) – to meet new physics goals, a central vertexing portion of the detector called SVX II was designed. It consists of double-sided silicon sensors with a combination of both 90-degree and small-angle stereo layers. The SVX II is nearly twice as long as the original SVX and SVX′ (96 cm instead of 51 cm), which were constrained to fit within a previous gas-based track detector (CTC) used

1969	ground breaking for National Accelerator Laboratory “Main Ring”
1972	200 GeV beam in the Main Ring
1983	first beam in the “Energy Doubler” $\Rightarrow$ “Tevatron”
1985	CDF observes first $p\overline{p}$ collisions
1988-89	**Run 0**, CDF collects $\sim$3 pb^{-1}
1992-93	**Run Ia**, CDF and DØ collect $\sim$20 pb^{-1}
1994-95	**Run Ib**, CDF and DØ collect $\sim$90 pb^{-1}
2001-02	**Run II** with new Main Injector and Recycler,
	upgraded CDF and DØ expect 2000 pb^{-1}=2 fb^{-1}
2003-2006(?)	**Run IIb, RunIII(?)**, 15-30 fb^{-1}

Table 2: *Some highlights in the history of the Fermilab Tevatron. This table lists primarily milestones associated with the collider program. In addition, there have been several Tevatron fixed-target runs, producing a wealth of physics results.*

to locate the position of interactions along the beam line. SVX II has 5 layers instead of 4 of the previous silicon detector and it is able to give 3-dimensional information on the tracks.
Intermediate Silicon Layer (ISL) is a large radius ($R = 29\ cm$) silicon tracker with a total active area of $\sim 3.5\ m^2$. It is composed of 296 basic units, called ladders, made of three silicon sensors bonded together in order to form one electric unit. Figure 2 (left) gives a schematic representation of the ISL detector. The ISL is located between the Silicon Vertex Detector and the Central Outer Chamber. Being at a distance of $\sim 23\ cm$ in the central part, from the beam-line, it covers a pseudorapidity region of $|\eta| < 1$.
A schematic view of the principal active components of the CDF Run II **silicon system** is given in Figure 2 (right).

- **Central Outer Tracker (COT)**
  COT is the new CDF central tracking chamber. It is an open cell drift chamber able to operate at a beam crossing time of 132 ns with a maximum drift time of $\sim$100 ns. The COT consists of 96 layers arranged in four axial and four stereo superlayers. It also provides dE/dx information for particle identification.

- **Time-of-Flight Detector (TOF)**
  New scintillator based Time-of-Flight detector has been added using a small space available between COT and solenoid. With its expected 100 ps time-of-flight resolution, the TOF system will enhance the capability to tag charged kaons in the p_T range from ~ 0.6 to few GeV/c as requested from the B physics program;

- **Plug Calorimeter**
  A new scintillating tile plug calorimeter has been realized in order to have a good electron identification up to $|\eta| = 2$.

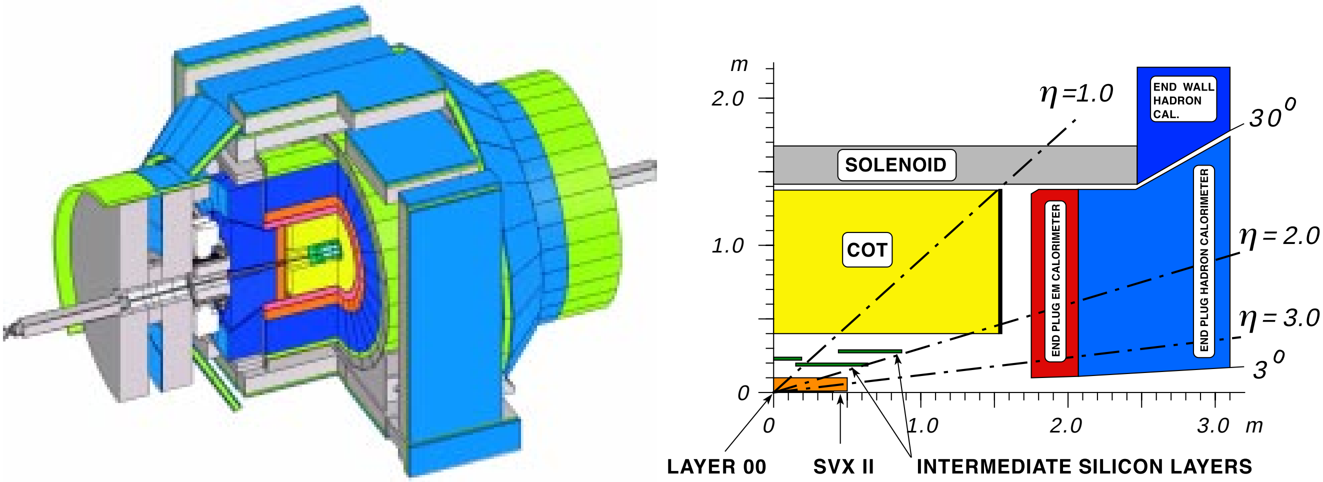

Figure 1: *(left) An overview of the Collider Detector at Fermilab (CDF) in its Run II configuration (CDF-II); (right) A cutaway view of one quadrant of the inner portion of the CDF-II detector showing the tracking region surrounded by the solenoid and endcap calorimeters.*

- **Muon system** has also been upgraded: the coverage in the central region has been almost doubled.
- A new **Data Acquisition System (DAQ)** has been adapted to short bunch spacing of 132 ns. It is capable to record data with event size of the order of 250 KB and permanent logging of 20 MB/s.

3 Run I results on Diffractive Physics

During the Run I the CDF Collaboration studied a large variety of diffractive processes. These analysis can be summarized as follow:

1. Dijets with rapidity gaps both at center of mass energy of $\sqrt{s} = 630\ GeV$ and 1.8 TeV [4, 5, 6];
2. Dijets with a leading antiproton at $\sqrt{s} = 630\ GeV$ and 1.8 TeV [7, 8];
3. Dijets production in Double Pomeron Exchange (DPE) [9];
4. Soft single-diffraction (SD) at $\sqrt{s} = 630\ GeV$ and at 1.8 TeV [10];
5. Soft double-diffraction (DD) at $\sqrt{s} = 630\ GeV$ and at 1.8 TeV [11];
6. W-boson diffractive production [12];
7. J/ψ diffractive production [13];

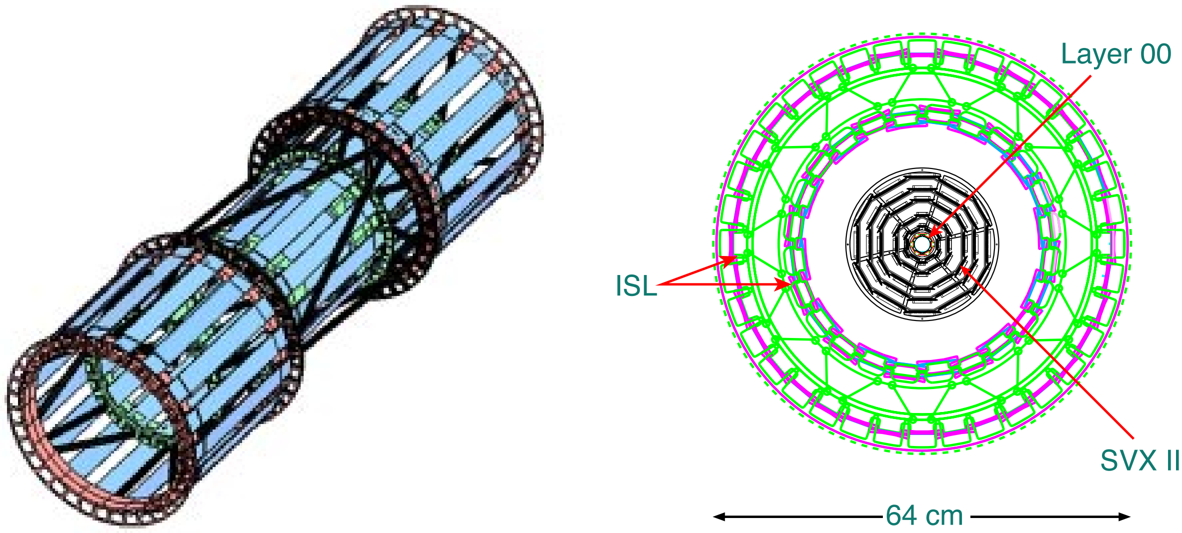

Figure 2: *(left) Schematic view of the the Intermediate Silicon Layers Detector; (right) a radial view of the CDF Run II silicon system.*

8. dijet and b-quark diffractive production [14, 15];

A typical signature of diffraction event at Tevatron is a leading proton or antiproton and/or a rapidity interval almost empty in tracks (*rapidity gap*). The di-jet production diagrams for single diffraction (SD), double diffraction (DD) and Pomeron exchange are summarized in Figure 3. The above studies confirm that the Regge factorization is violated in soft single and double diffraction; this violation leads to a scaling behavior expressed as s-independence of the M^2 distribution of the differential cross sections. The data for both SD and DD are in agreement with the renormalized gap model (see Figure 4).
In the case of hard diffraction a severe breakdown of factorization is observed, expressed as a suppression of the the diffractive to non-diffractive production rates relative to predictions from Regge-type models based on factorization or from diffractive parton densities measured at HERA. The suppression factor is approximately equal to that observed in soft diffraction. The diffractive to non-diffractive production rates are approximately flavor independent.

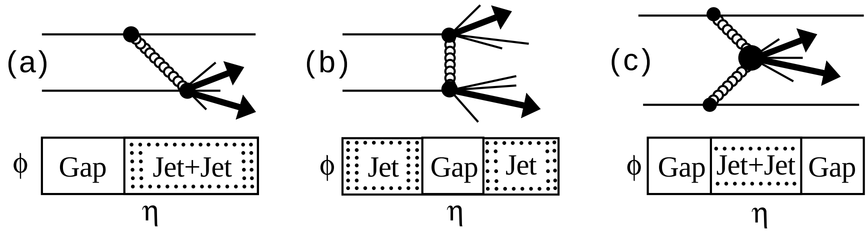

Figure 3: Dijet production diagrams and event topologies for (a) single-diffraction, (b) double-diffraction, and (c) double Pomeron exchange.

4 B Physics

Even if, at present, there are dedicated machines (B-factories) that are doing important studies on B physics, there are plenty of good reasons to do the same at Tevatron collider. B physics is important because it is an extraordinary laboratory to test several fundamental aspects of the Standard Model (SM). At Tevatron the production cross section is really large i.e. at the expected Run II luminosity the $b\bar{b}$ production rate will be $\sim 10^{11}$ events/year. Moreover, only at hadron colliders it is possible to produce all B species. In fact, at B-factories only light-Bs are within the reach. The enormous statistics that CDF and DØ plan to accumulate will allow us to study various B decays modes, search for CP violation and $B_{d,s}$ mixing. The main goals of the CDF B physics program are to provide a precision measurement of the angle $\sin(2\beta)$ of the unitary triangle, as well as to exploit the B_s^0 and B_c^+ mesons and b baryons, which will be a unique feature of hadron colliders.
During the Run I, CDF has been the first experiment where $\sin(2\beta)$ has been measured [16]. This relevant quantity is expected to be measured with an uncertainty of 0.072 under the pessimistic assumption that $\sin(2\beta) = 1$. We believe that this uncertainty is overestimated. In fact, this number has been obtained without taking into account the increased di-lepton bandwidth and the fact that the number of expected J/ψ per nb^{-1} is almost 2.8 times the previous one. Flavor tagging efficiency is the key feature of most of the Tevatron B physics analysis. In table 3 we summarize the tagging capabilities (εD^2) for Tevatron experiments.

Tag Strategy	εD^2(%) CDF RUN I	εD^2(%) CDF RUN II	εD^2(%) DØ RUN II
Same Side	$1.8 \pm 0.4 \pm 0.3$	2	2
Soft Lepton	$0.9 \pm 0.1 \pm 0.1$	1.7	3.1
Jet Charge	$0.8 \pm 0.1 \pm 0.1$	3	4.7
Opp. Side	none	2.4	none

Table 3: *Flavor tagging efficiencies for both CDF and DØ detectors based on knowledge from Run I and MC studies.*

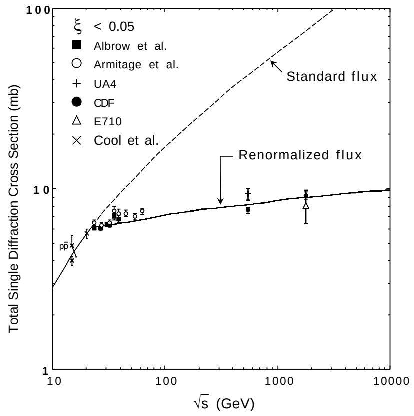

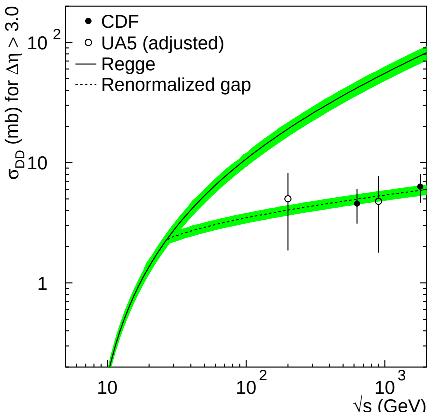

Figure 4: *The total single σ^t_{SD} (left) and double σ^t_{DD} (right) diffraction cross sections for $pp\,(\bar{p}p)$ scattering versus $\sqrt{s}$ compared with different theory predictions.*

5 Single Top quark production

Even if the dominant process for top quark is $t\bar{t}$ pair production, a top quark can be also produced alone, in association with a b quark, through the electroweak interaction [17]. The two dominant "single-top" processes are "Wg"(i.e. W-gluon fusion, $qg \to t\bar{b}q'$) and "$W^\star$" ($q\bar{q}' \to t\bar{b}$). Within the context of the standard model, a measurement of the rate of these processes at a hadron collider allows a determination of the Cabibbo-Kobayashi-Maskawa matrix element V_{tb} [18]. Because of significant differences in the final-state kinematics of the two single-top processes, it is possible to search for them separately.

CDF searched for single top production using all the Run I data sample ($106 \pm 4\ pb^{-1}$). The events have been selected by requiring an isolated [19] electron (muon) candidate with E^e_T (p^μ_T) > 20 GeV (GeV/c) and missing transverse energy $\not{E}_{\rm T} > 20$ GeV from the neutrino [20]. Events identified in the previous CDF analysis [21] as $t\bar{t}$ dilepton candidates have been removed from the sample. Events with a second lepton having same-flavor and opposite-charge as well as an invariant mass with the first lepton ranging between 75 and 105 GeV/c^2 are rejected as likely originated from Z^0 boson decays. Furthermore, to reject those dilepton events coming from $t\bar{t}$ or Z^0, where one lepton fails our electron or muon identification, we remove events which contain a track with (1) $p_T > 15$ GeV/c, (2) a charge opposite to that of the primary lepton, (3) the total p_T of all tracks in a cone of radius $\Delta R \equiv \sqrt{\Delta\eta^2 + \Delta\phi^2} = 0.4$ around this track is less than 2 GeV/c [22]. Jets are formed as clusters of calorimeter towers within cones of fixed radius $\Delta R = 0.4$. Events are required to have one, two, or three jets with $E_T > 15$ GeV and $|\eta| < 2.0$; at least one jet must be identified as likely to contain a b quark ("b-tagged") using displaced-vertex information from the silicon vertex detector (SVX) [22].

To measure the combined $Wg + W^\star$ single-top production cross section, we use a kinematic variable with distribution which is very similar for the two single-top processes and is different for background processes: the scalar sum H_T of $\not{E}_{\rm T}$ and the transverse energies of the lepton

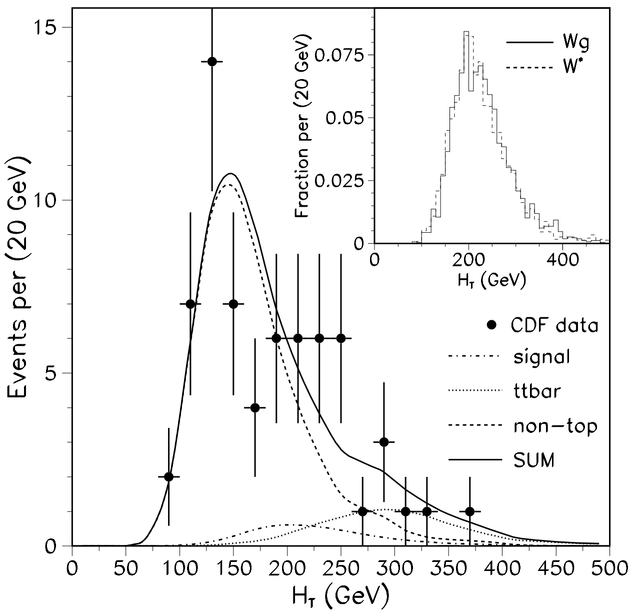

Figure 5: *H_T distribution for data in the combined search, compared with smoothed Monte Carlo predictions for signal and backgrounds.*

and all jets in the event.
The result of the maximum-likelihood fit for the single-top content of the data is $-0.6^{+4.8}_{-4.0}$ for Wg events and $7.6^{+5.9}_{-4.8}$ for $W^\star$ events. These results translated in 95% C.L. upper limit on the single top quark cross sections give an upper limit of 13 *pb* on single-top production in the Wg channel and 18 *pb* in the W^* channel.
The increase in the center of mass energy as well as the integrated luminosity in the Run II will provide $\sim$ 40-50 times more $t\bar{t}$ events than in Run I. In addition to a large reduction in statistical uncertainties, systematic uncertainties such as the jet energy scale and MC modelling will also be reduced. Given the size of the Run 2 data sample, we have made projections for the precision we can expect for a variety of measurements. Some of these projections are given in Table 4. Run 2 and a future Run 3 will clearly provide very rich top samples with which to probe the SM and physics beyond it.

6 Higgs at Tevatron

At Tevatron the Higgs boson is expected to be produced via gluon fusion or associated with W or Z bosons. The Higgs production cross section for different channels is given in Figure 6.a [23]. Although the gluon fusion mode is expected to give the most important contribution to the Higgs production, it will be overwhelmed by the large QCD background. Therefore, given sufficient luminosity, the most promising SM Higgs discovery mechanism for $m_H < 130\ GeV$ consists of $q\bar{q}$ annihilation into a virtual V^* ($V = W$ or Z), where the vitual $V^* \to Vh_{SM}$ followed by $h_{SM} \to b\bar{b}$ and the leptonic decay of the V that will

Measurement	Precision (in Run II)
M_{Top}	1.5%
$\sigma(p\bar{p} \to t\bar{t})$	9%
Single Top quark cross section	24%
V_{tb} (from Single Top)	13%
F_0	5.5%
$\sigma * BR(X \to t\bar{t})$	0.1 pb at 1 TeV
$BR(t \to \gamma c)$	$< 2.8 \times 10^{-3}$
$BR(t \to Zc)$	$< 1.3 \times 10^{-2}$
$BR(t \to Hb)$	$< 12\%$

Table 4: *Expected precision for top quark measurements assuming an integrated luminosity of* $\int \mathcal{L} = 2\ fb^{-1}$.

serve as a trigger. The main background for this mode will be $Wb\bar{b}$ and WZ processes. For $m_H \sim 120 - 190$ GeV, where the Higgs is produced with a vector bosons, it will mainly decay into W^*W^* states with subsequent decay $(W, Z)W^*W^* \to \ell^\pm\nu\ell^\pm\nu jj$. For this case selection criteria requires two leptons with $p_T \geq 10$ GeV having the same charge and two separate jets with $p_T \geq 15$ GeV and at least 10 $GeV\ \not{E}_T$. The main background in this case is $WZjj$ production. Among various analyses underway some interesting result could also come from the use of neural networks techniques. The integrated luminosity required per each Tevatron experiment, to either exclude a SM Higgs boson at 95% C.L. or discover it at the 3σ or 5σ level, as a function of the Higgs mass is given in Figure 7. The curves shown are obtained combining the several analysis studied for the different mass regions.

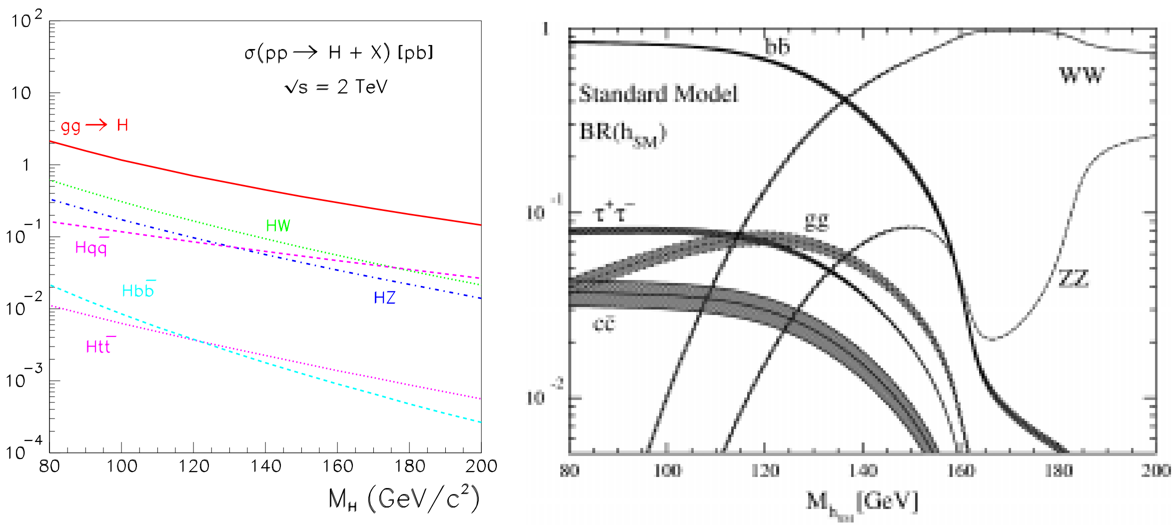

Figure 6: *(left) The SM Higgs production cross section at Tevatron; (right) Higgs decay branching fractions as function of mass.*

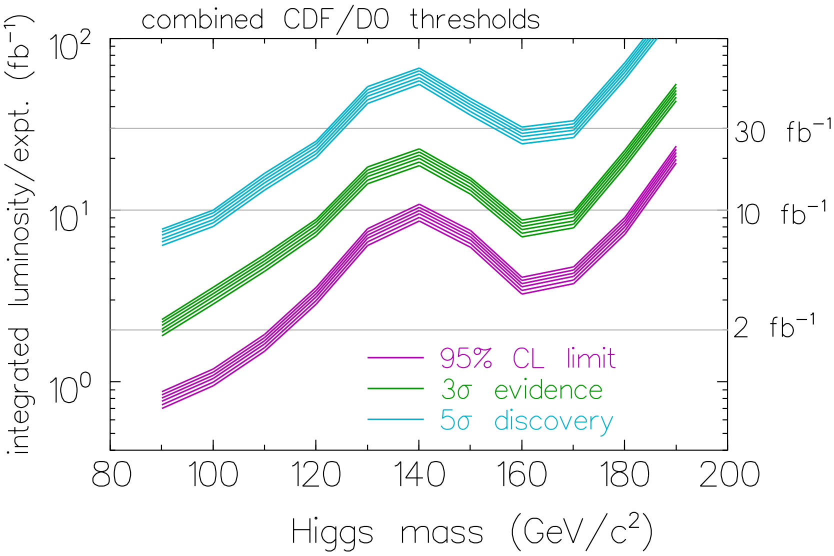

Figure 7: *Integrated luminosity delivered per experiment required to either exclude at 95% C. L. (bottom curve) or discover the SM Higgs at the* 3σ *(middle curve) or* 5σ *(top curve) level as a function of Higgs mass. The theoretial uncertainties are already included in all curves.*

7 Search for Physics beyond the SM

7.1 Supersymmetry

7.1.1 Introduction

Although, at present, the Standard Model (SM) provides a remarkably successful description of known phenomena, there are plenty of aspects that we do not understand yet and that may suggest the SM to be most likely a low energy effective theory of spin-1/2 matter fermions interacting via spin-1 gauge bosons [24]. An excellent candidate to a new theory, able to describe physics at arbitrarily high energies, is Supersymmetry (SUSY). SUSY is a large class of theoretical models based on the common assumption that there exist in nature a fermion-boson symmetry. A comprehensive SUSY search is almost impossible because of the large amount of truly independent parameters. The strategy is then to search for signals suggested by particular models in which theoretical assumptions are also adopted to reduce the number of free parameters to a few. In Supersymmetry fermions can couple to a sfermion and a fermion, violating lepton and/or baryon number. To avoid this problem, a discrete multiplicative quantum number, the $\mathcal{R}$-parity was introduced [25]: $\mathcal{R} \equiv (-1)^{3B+L+2S}$. SUSY models can be constructed assuming either conservation or violation of this quantum number (RPV).

7.1.2 Search for third generation scalar quarks

Search for scalar top squark is particularly interesting as the strong Yukawa coupling between top/stop and Higgs fields give rise to potentially large mixing effects and mass splitting. Such effects can lead the lightest top-squark mass eigenstate $\tilde{t}_1$ to be lighter than the other squarks:

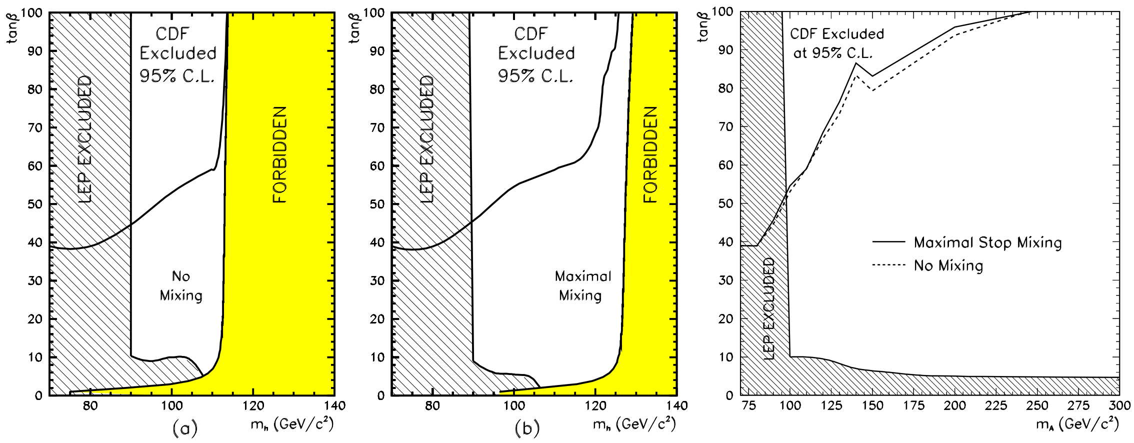

Figure 8: *(left) 95% C.L. exclusion region in the m_h versus tan(β) plane from CDF MSSM neutral Higgs search; (right) and m_A versus tan(β).*

$m_{\tilde{t}_1} < m_{\tilde{q}}$ [26]. When a set of SUSY parameters such as A, μ and $\tan(\beta)$ [27] is suitably tuned, light bottom squarks may also occur.
Both the CDF and DØ experiments have searched for direct stop quark pair production: $p\bar{p} \rightarrow \tilde{t}_1\bar{\tilde{t}}_1$ with $\tilde{t}_1$ decaying into the following channels: $\tilde{t}_1 \rightarrow b\tilde{\chi}_1^{\pm}$, $\tilde{t}_1 \rightarrow b\ell^+\tilde{\nu}$ [28] and $\tilde{t}_1 \rightarrow c\tilde{\chi}_1^0$ [29]. CDF has also searched for indirect stop quark production trough the top quark decay: $t \rightarrow \tilde{t}_1\tilde{\chi}^0$ with $\tilde{t}_1 \rightarrow b\chi_1^{\pm}$ [30]. Searches for direct scalar bottom production $p\bar{p} \rightarrow \tilde{b}_1\bar{\tilde{b}}_1$ with the sbottom decaying into: $\tilde{b}_1 \rightarrow b\tilde{\chi}_1^0$ have been performed from both Tevatron Experiments [29, 31]. An overview on such results can be found in [32].

7.1.3 Search for RPV stop decays

CDF searched for a pair produced scalar top squark decaying via non-zero $\mathcal{R}$-parity violating coupling λ'_{333} to $\tilde{t}_1 \rightarrow \tau b$ [33]. The experimental signature of this process is two τ leptons and two b quarks in the final state. Events have been selected by requiring a lepton (e or μ) from $\tau \rightarrow \ell\nu_\ell\nu_\tau$, a hadronically decaying tau lepton and two jets. The principal background processes are $Z \rightarrow \tau^+\tau^-$, W+jets, $t\bar{t}$, Drell-Yan and diboson events. We observed, combining both the muon $\tilde{t}_1\bar{\tilde{t}}_1 \rightarrow \tau^+\tau^- b\bar{b} \rightarrow \mu\tau_h b\bar{b} + X$ and the electron channel $\tilde{t}_1\bar{\tilde{t}}_1 \rightarrow \tau^+\tau^- b\bar{b} \rightarrow e\tau_h b\bar{b} + X$, that no events passed the selection cuts. This is consistent with the expected SM background of 1.92 ± 0.19 events in the electron channel and 1.13 ± 0.14 in the muon channel. A 95% *C.L.* lower limit on the stop quark mass have been set: $m_{\tilde{t}_1} > 119$ GeV/c^2, for a dominant λ'_{333} coupling. The more recent and competitive result on the lower limit of the stop mass with this signature comes from ALEPH/LEP experiment [34].

7.1.4 Search for MSSM neutral Higgs

The Minimal Supersymmetric Standard Model (MSSM) predicts five physical Higgs bosons: a charged pair (H^+, H^-), two CP-even scalars (h^0, H^0) and a CP-odd (A^0). CDF has

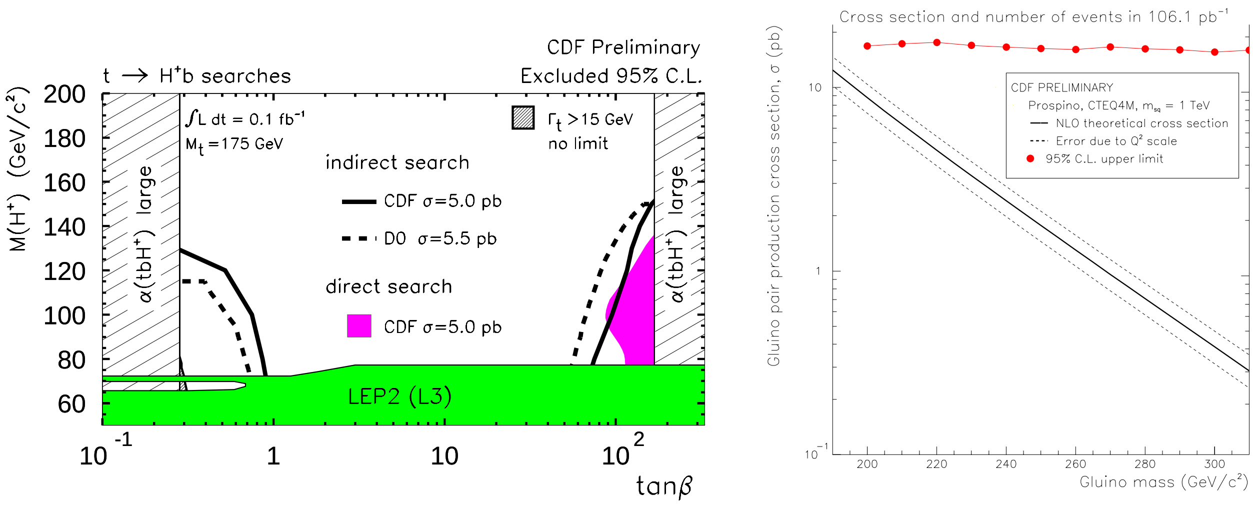

Figure 9: *(left) 95% C.L. exclusion region in the tan(β) versus $m_{H^\pm}$ plane for the charged Higgs searches from CDF and DØ; (right) 95% C.L.upper limit on the gluino production cross section as a function of $\tilde{g}$ mass using the like-sign top dilepton sample.*

searched for a neutral MSSM Higgs ϕ, where ϕ means h or H or A, produced in association with $b\bar{b}$: $p\bar{p} \to b\bar{b}\phi \to b\bar{b}b\bar{b}$. The analysis is based on on 91 pb^{-1} of data corresponding to the Run 1B multijet sample. With basic parameter choices for both the SUSY scale and the stop mixing, we obtained a 95% C.L. on the lower mass value for ϕ in a region of SUSY parameter space where: tan$\beta > 30$. These results are summarized in Fig. 8.

7.1.5 Search for charged Higgs in the top quark decay

The charged Higgs particle ($H^\pm$) may be observed through the following top quark decay: $t \to H^+b \to \tau^+\nu b$. This process is favored over the SM one: $t \to Wb$ if $\mathrm{m}_{H^\pm} < (m_t - m_H)$ in two separate tan(β) regions: tan(β)< 1 and tan(β)> 70 [35].
Both CDF and DØ searched for charged Higgs. In particular the CDF direct search was performed requiring a high-P_T central lepton ($|\eta| < 1$, $p_T^\ell > 20$ GeV, $\ell = e$ or μ) as well as a central τ lepton with $p_T^\tau > 15$ GeV, 2 jets and missing transverse energy ($\not{E}_\mathrm{T}$) with significance: $S_{\not{E}_T} \equiv \not{E}_\mathrm{T}/\sqrt{\sum E_T} > 3$ GeV$^{1/2}$. Better results have been obtained both from CDF and DØ performing an indirect search based on the suppression of SM $t\bar{t} \to W^+W^-b\bar{b}$ decays caused by the presence of the competitive channel $t \to H^+b$. Fig. 9 (left) show the 95% C.L. excluded region as a function of tan(β).

7.1.6 Search for gluino pair production using LS top events

CDF recently searched for gluino pair production using like-sign (LS) top events. The analysis have been performed using 106.1 pb^{-1} of Run I data. In the SUSY model under study the scalar top squark is not only the lightest squark but also the only one lighter than gluino and satisfy the condition: $m_t + m_{\tilde{t}_1} < m_{\tilde{g}}$. Therefore $\tilde{g} \to t\tilde{t}$ is the preferred decay channel and because of the Majorana nature of gluinos they give rise to LS top quarks from

$\tilde{g}\tilde{g}$ decays. In order to search for such events CDF used the top dilepton events. The results of this search are shown in Fig. 9 (right); no mass limits have been set due to the presence of three signal events and to the inability to probe gluino masses in the region close to the top mass, where the stop mass is forced to be unreasonably light.

7.2 Extra Dimensions

Motivated in part by naturalness issues, numerous scenarios have emerged recently, that address the hierarchy problem within the context of the old idea that some part of the physical world (i.e. the SM-world) is confined to a brane in a higher dimensional space [36]. Although supergravity theories were formulated up to 11 dimensions and Superstring theories in 10 dimensions were known since the 70's, the idea to extend this extra spatial dimension paradigm (ESD) to other contexts, received a new impulse only recently [37]. As we don't experience in our everyday world, more then 3 spatial dimensions, we have to assume that any possible ESD is hidden. There is a simple and elegant way to hide possible extra spatial dimensions: the *compactification*. The result is achieved by assuming, for example, that the extra dimensions form, at each point of the 4$-$dimensional space, a torus of volume $(2\pi)^{\mathcal{D}}R_1R_2...R_{\mathcal{D}}$. In this way it is possible to allow the gravity to live in the $\mathcal{D}$ large extra dimensions, the *bulk*, while the SM fields will lie on a 3-$\mathcal{D}$ surface, the *brane*.

The large extra dimension scenario (LED) started with the works of Arkani-Hamed, Dimopoulos and Dvali (ADD) [37, 38]. In this model the SM particles live on a $3+1-$dimensional space ($3-$brane) while the gravity is free to propagate in higher-dimensional space, extra dimensions. This model predicts essentially the emission and exchange of large Kaluza-Klein towers of gravitons that are finely-spaced in mass. The ADD Model was first proposed to solve the hierarchy problem by requiring the compactified dimensions to be of very large size. Most of the searches performed until now for large extra dimensions have been done assuming the ADD phenomenology. We summarize here signatures and results of such searches.

As Kaluza-Klein gravitons couple to the momentum tensor, they therefore contribute to most of the SM processes. Depending on whether the G_{KK} leaves our world or remains virtual, the collider signatures change. For graviton that propagate in the bulk, in particular, from the point of view of our $3+1$ space-time, energy and momentum are not conserved in the G_{KK} emission. Gravitons, on the other hand, interacting weakly with detectors, escape detection causing a typical missing transverse energy ($\not{E}_{\mathrm{T}}$) signal. The virtual exchange of graviton towers either leads to modifications in SM cross sections and asymmetries or to new processes not allowed in the SM at the tree level. Collider signatures with virtual exchanges of $KK-$gravitons are several and include diphoton, diboson and fermion-pair production. In the case of virtual G_{KK} emission, gravitons lead to apparent violation of 4-momentum as well as of the angular momentum. The impact of virtual gravitons at Tevatron collider can be observed in processes such as: $q\bar{q} \to G \to \gamma\gamma$ or $gg \to G \to e^+e^-$ where the ADD model introduces production mechanism that can increase the cross-section of diphoton and dielectron production at high invariant mass over the SM. The diphoton and dielectron

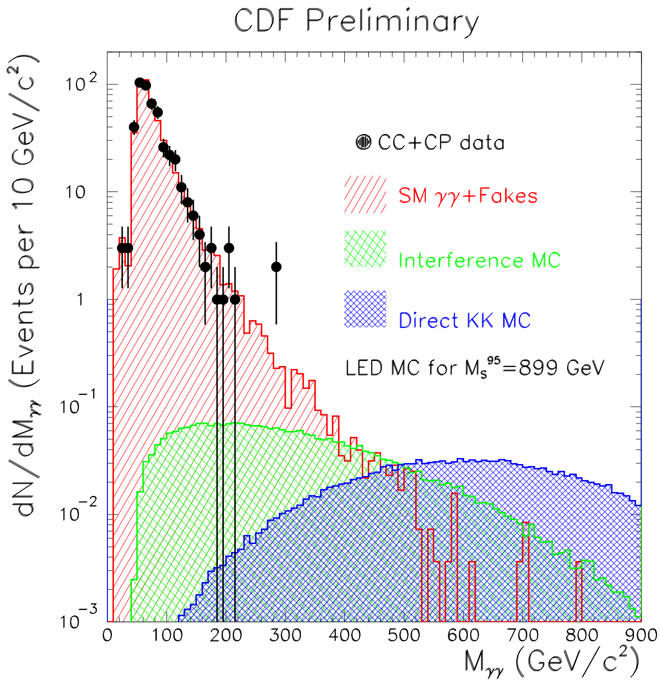

Figure 10: *Comparison of Data with Monte Carlo assuming* $M_s = 899$ *GeV; the different curves show the different contributions to the diphoton masses.*

cross-section considering the LED contributions take the form [38]:

$$\frac{d^2\sigma_{Tot}}{dcos\theta^*\ dM} = \frac{d^2\sigma_{SM}}{dcos\theta^*\ dM} + \frac{a(n)}{M_{\mathcal{F}}^4}\ F_1(cos\theta^*, M) + \frac{b(n)}{M_{\mathcal{F}}^8}\ F_2(cos\theta^*, M) \qquad (1)$$

where $cos\theta^*$ is the scattering angle of the photon or electron in the center of mass frame of the incoming parton. The first term in the expression 1 is the pure SM contribution to the cross section; the second and the third part are the interference term and the direct G_{KK} contribution. The characteristic signatures for contributions from virtual G_{KK} correspond to the formation of massive systems abnormally beyond the SM expectations. Figure 10 shows a comparison of the di-photon Mass ($M_{\gamma\gamma}$) for the SM background processes, for the direct KK term and for the interference term. With no excess apparent beyond expectations of the SM, CDF proceeds to calculate a lower limit on the graviton contribution to the di-EM cross section. This limits expressed in the Hewett notation are for combining the central and central plug photons and electrons analysis: $M_{\mathcal{F}} > 899$ GeV for $\lambda = -1$ and $M_{\mathcal{F}} > 797$ GeV for $\lambda = +1$. For the central-central electrons only the limits are $M_{\mathcal{F}} > 855$ GeV for $\lambda = -1$ and $M_{\mathcal{F}} > 840$ GeV for $\lambda = +1$.

8 Conclusions

We presented a sample of the latest updated results on some of the many topics explored at CDF in the recent years. In particular, results on diffraction processes, b-physics, single-top production, Higgs searches and searches for physics beyond the Standard using the full Run I data sample has been discussed. With the Run II upgrades, providing an approximately 20-fold increase in luminosity and improved detector performance, we expect these results to be greatly extended.

9 Acknowledgments

I wish to thank Khazret Nirov and the Organizers of the XI-th International School "Particles and Cosmology" for the excellent conference and for their kind hospitality.

References

[1] F. Abe *et al.* (CDF Collaboration), The CDF-II detector: Technical design report, FERMILAB-PUB-96-390-E (1996).

[2] T. LeCompte, Ann. Rev. Nucl. Part. Sci. **50**, 71-117 (2000);

[3] F. Abe *et al.* (CDF Collaboration), Nucl. Instrum. Meth. **A271**, 387-403 (1988).

[4] F. Abe *et al.*, Phys. Rev. Lett. **80**, 1156 (1998); **81**, 5278 (1998).

[5] F. Abe *et al.*, Phys. Rev. Lett. **74**, 855 (1995).

[6] F. Abe *et al.*, Phys. Rev. Lett. **80**, 1156 (1998).

[7] *Diffractive dijet production at* $\sqrt{s} = 630$ *and 1800 GeV at the Fermilab Tevatron*, CDF Collaboration, to be submitted to Phys. Rev. Letters.

[8] T. Affolder *et al.*, Phys. Rev. Lett. **84**, 5043 (2000).

[9] T. Affolder *et al.*, Phys. Rev. Lett. **85**, 4215 (2000).

[10] F. Abe *et al.*, Phys. Rev. D **50**, 5535 (1994).

[11] *Double diffraction dissociation at the Fermilab Tevatron collider*, CDF Collaboration, accepted by Phys. Rev. Letters.

[12] F. Abe *et al.*, Phys. Rev. Lett. **78**, 2698 (1997).

[13] *Observation of diffractive* J/ψ *production at the Fermilab Tevatron*, CDF Collaboration, submitted to Phys. Rev. Letters.

[14] F. Abe *et al.*, Phys. Rev. Lett. **79**, 2636 (1997).

[15] T. Affolder *et al.*, Phys. Rev. Lett. **84**, 232 (2000).

[16] F. Abe *et al.* (CDF Collaboration), Phys. Rev. D **61**, 072005 (2000).

[17] S. S. D. Willenbrock and D. A. Dicus, Phys. Rev. D **34**, 155 (1986); S. Dawson and S. Willenbrock, Nucl. Phys. B **284**, 449 (1987); C.-P. Yuan, Phys. Rev. D **41**, 42 (1990); R. K. Ellis and S. Parke, Phys. Rev. D **46**, 3785 (1992); D. Carlson and C.-P. Yuan, Phys. Lett. B **306**, 386 (1993).

[18] T. Stelzer and S. Willenbrock, Phys. Lett. B **357**, 125 (1995).

[19] A lepton is "isolated" if the non-lepton E_T in an η-ϕ cone of radius 0.4 centered on the lepton is less than 10% of the lepton's E_T or P_T.

[20] Missing transverse energy $\not{E}_{\rm T}$ is defined as the magnitude of $-\sum_i E_T^i \hat{n}_i$, where $\hat{n}_i$ is a unit vector in the azimuthal plane that points from the beamline to the ith calorimeter tower.

[21] CDF Collaboration, F. Abe *et al.*, Phys. Rev. Lett. **80**, 2779 (1998).

[22] CDF Collaboration, F. Abe *et al.*, Phys. Rev. Lett. **79**, 3819 (1997).

[23] M. Spira, hep-ph/9810289.

[24] G. Altarelli, CERN-TH-98-348, hep-ph/9811456 (1998).

[25] H. Dreiner, *Pramana* **51**, 123 (1998).

[26] K. Hikasa and M. Kobayashi, Phys. Rev. D **36**, 724 (1987).

[27] The definition of these parameters can be found for example in the paper: D. I. Kazakov, Beyond the standard model (in search of SUSY), hep-ph/0012288 *Proceedings of the European School on High Energy Physics, 2000.*

[28] T. Affolder *et al.* [CDF Collaboration], Phys. Rev. Lett. **84**, 5273 (2000).

[29] S. Abachi *et al.* [D0 Collaboration], Phys. Rev. Lett. **76**, 2222 (1996).
T. Affolder *et al.* [CDF Collaboration], Phys. Rev. Lett. **84**, 5704 (2000).

[30] T. Affolder *et al.* [CDF Collaboration], Phys. Rev. D **63**, 091101 (2001).

[31] B. Abbott *et al.* [D0 Collaboration], Phys. Rev. D **60**, 031101 (1999)

[32] C. Pagliarone, *Proceedings of 13th Topical Conference on Hadron Collider Physics*, Mumbai, 14-20 Jan 1999; FERMILAB-CONF-99-062-E.
C. Pagliarone, *Proceedings of Crimean Summer School-Seminar on New Trends in High-Energy Physics*, Crimea, 27 May - 4 Jun 2000; FERMILAB-CONF-00-217-E.

[33] W. Porod, D. Restrepo and J. W. Valle, hep-ph/0001033.

[34] R. Barate *et al.* [ALEPH Collaboration], Eur. Phys. J. C **19**, 415 (2001).

[35] M. Drees and D. P. Roy, Phys. Lett. B **269**, 155 (1991).
D. P. Roy, Phys. Lett. B **283**, 403 (1992).

[36] T. Kaluza, Sitzungober, Preuss. Akd. Wiss. Berlin, p.966 (1921);
O. Klein, Z. Phys. **37**, 895 (1926).

[37] N. Arkani-Hamed, S. Dimopoulos and G. Dvali, Phys. Lett. B**249**, 263 (1998);

[38] N. Arkani-Hamed, S. Dimopoulos and G. Dvali, Phys. Lett. B**436**, 257 (1998), Phys. Lett. D**59**, 257 (1999).

[39] G. F. Giudice, R. Rattazzi and J. D. Wells, Nucl. Phys. B **544**, 3 (1999)

[40] T. Han, J. D. Lykken and R. J. Zhang, Phys. Rev. D **59**, 105006 (1999)

[41] J. L. Hewett, Phys. Rev. Lett. **82**, 4765 (1999)